*Chemical Product and Process Modeling*

*Volume* 2, *Issue* 3 2007 *Article* 8

# Molecular Simulation Study of Vapor-Liquid Equilibrium of Morse Fluids

**Sang Kyu Kwak,** *Nanyang Technological University*
**Jayant K. Singh,** *Indian Institute of Technology Kanpur*
**Jhumpa Adhikari,** *Indian Institute of Technology Bombay*

**Recommended Citation:**
Kwak, Sang Kyu; Singh, Jayant K.; and Adhikari, Jhumpa (2007) "Molecular Simulation Study of Vapor-Liquid Equilibrium of Morse Fluids," *Chemical Product and Process Modeling*: Vol. 2: Iss. 3, Article 8.
**DOI:** 10.2202/1934-2659.1097

# Molecular Simulation Study of Vapor-Liquid Equilibrium of Morse Fluids

Sang Kyu Kwak, Jayant K. Singh, and Jhumpa Adhikari

## Abstract

The Morse potential energy function (PEF) is considered regarding the characterization of interaction forces of particles with tuning parameters. Phase coexistence of Morse fluids is predicted for different steepness and range of the PEF parameters using the grand-canonical transition matrix Monte Carlo (GC-TMMC) method, with quantification of the parameter *S*, which is the product of a constant with a unit of reciprocal length and the equilibrium distance between two molecules. We found that a lower limit of *S* exists bounded by infinite critical temperature. The critical properties of the vapor-liquid equilibrium curves are estimated using a rectilinear diameter method and a scaling law approach. A Clausius-Clayperon type relation of *S* and critical temperature is derived in this work. Vapor-liquid surface tension of Morse fluids by finite size scaling and GC-TMMC is also reported. Surface tensions are found to be higher at lower *S*.

**KEYWORDS:** molecular simulation, Morse potential, critical properties, grand-canonical transition matrix Monte Carlo

**Author Notes:** This work has been presented in the Regional Symposium on Chemical Engineering, Singapore, 2006, and we thank the conference secretariat, Dr. Xu Rong, for helping us to publish this work. We acknowledge that computational resources have been provided by the Computer Center at the Indian Institute of Technology, Kanpur and the School of Chemical and Biomedical Engineering at Nanyang Technological University, Singapore. The work was supported by Nanyang Technological University (Grant No.: NTU-SUG:M58120005).

## INTRODUCTION

In recognition of the degree of resemblance of the model system to the real one, the choice of the potential model is one of the most important factors. Particularly, Morse potential energy function (PEF), which has been developed about 70 some years ago (Morse, 1929), became attractive in the field of the theoretical chemistry due to closeness of description on the interaction forces of many body systems. Its robust characteristics allow investigating built-model systems such as diatomic molecules and metal components (Keyes, 1958; Girifalco and Weizer, 1959; Lincoln *et al*., 1967; Ruffa, 1981); small changes of parameters can easily transform one type of Morse PEF into another. The Morse PEF has the following formalism,

$$U(r_{ij})/D = \left[ e^{-2\alpha(r_{ij}-r_0)} - 2e^{-\alpha(r_{ij}-r_0)} \right] = \left[ e^{-2S(r_{ij}/r_0-1)} - 2e^{-S(r_{ij}/r_0-1)} \right] \quad (1)$$

where $r_{ij}$ is the distance of two molecules denoted as $i$ and $j$, $D$ is the dissociation energy, $\alpha$ is an adjustable constant with units of reciprocal length, and $r_0$ is the distance of two molecules in equilibrium. Note that we denote the parameter $\alpha r_0$ as $S$ hereafter. Figure 1 shows the schematic of Eq. (1) with different $S$ of which value of $r_0$ is unity in this study.

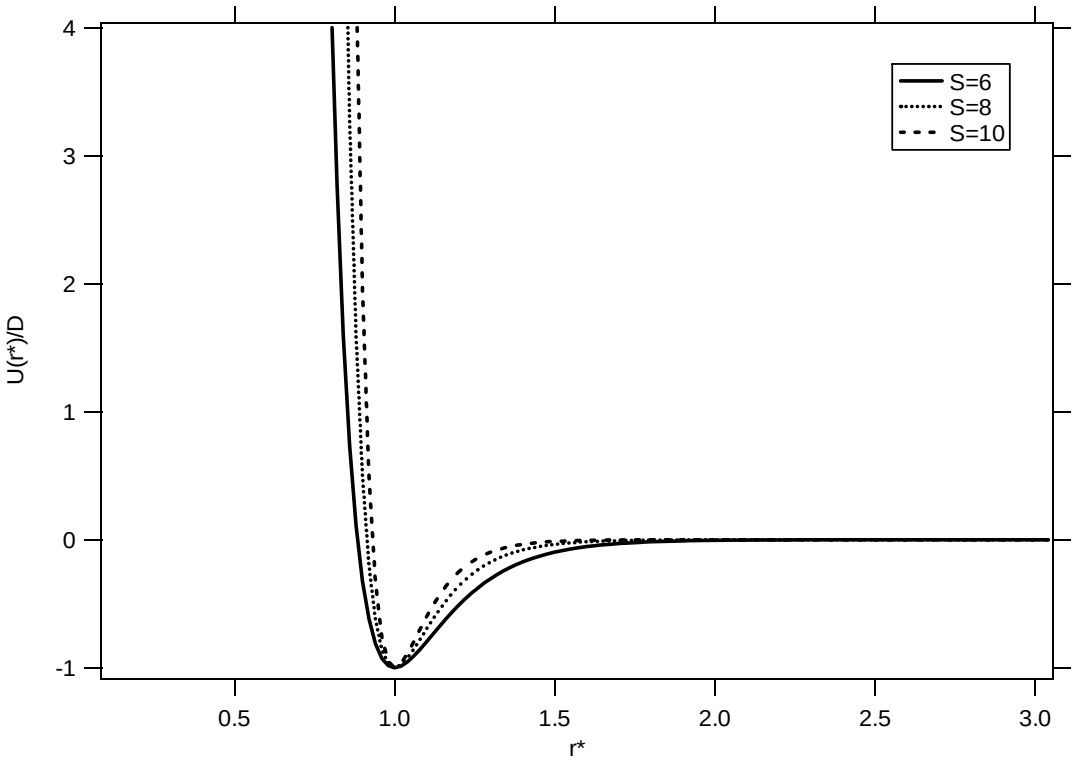


Figure 1. Plot of reduced interaction energy vs. relative distance, where $r^*$ is $r/r_0$.

The Morse PEF has been shown successfully to predict thermodynamic properties within confidence limits compared to experimental results. Recent study (Singh *et al*., 2006) shows a good agreement of vapor-liquid equilibrium (VLE) data including critical properties of metal components (e.g. Na, K, Al, Au and Cu) with parameters produced by a fitting procedure (Lincoln *et al*., 1967), yet with somewhat limited ranges of steepness and width of potential well. Note that aforementioned works from other authors are not beyond this regime of steepness and width. In this regard, our aim is to build a landscape of phase equilibria of the Morse PEF systems in lieu of corresponding state theorem in terms of *S*. Also, we map the value of *S* as the measurement of range and show the various VLE data with prediction of critical properties as well as surface tensions.

## SIMULATION

### Theoretical Approach

The grand canonical transition matrix Monte Carlo(GC-TMMC) method (Errington, 2003) is implemented to perform the simulations of the systems restricted with fixed properties of the chemical potential $\mu$, volume $V$, and temperature $T$. Note that the number of molecules (density) of the system varies. Analysis of statistical mechanics reveals the details of connectivity from microstates to a macrostate in the grand canonical scheme as follows,

$$\pi_s = \frac{1}{\Xi}\frac{V^{N_s}}{\Lambda^{3N_s}N_s!}\exp\left[-\beta(U_s-\mu N_s)\right] \tag{2}$$

The microstate probability $\pi_S$ of observing a system $s$ with energy $U_S$ and molecule number $N_S$ is shown in Eq.(2), where $\beta=1/k_BT$ is the inverse temperature with Bolzmann's constant $k_B$, $\Xi$ is the grand canonical partition function, and $\Lambda$ is the de Broglie wavelength. Eq.(2) is utilized to obtain the macrostate probabilities $\Pi(N)$'s, which are the collections of all the microstates for each of series of fixed number of molecules (e.g $\Pi(0) = \sum\pi_s(0)$, $\Pi(1) = \sum\pi_s(1)$, $\Pi(2) = \sum\pi_s(2)$, …). The probability distribution function is subsequently used to obtain the chemical potential of the coexistence phase through the histogram reweighting method developed by Ferrenberg and Swendson, 1988. The basic idea of the method is shown for a fixed $N$ as follows,

$$\ln\Pi(N;\mu) = \ln\Pi(N;\mu_0) + \beta N(\mu-\mu_0) \tag{3}$$

where $\mu_0$ is the user-input value of the chemical potential of the simulated system. The target chemical potential is located at the point, where the probability distribution function shows the equal area under vapor and liquid regions. Once the chemical potential is evaluated, the saturation pressure is determined by the following formula,

DOI: 10.2202/1934-2659.1097 

$$\beta pV = \ln\left(\sum_N \Pi(N)/\Pi(0)\right) - \ln(2) \tag{4}$$

The bridge function for the pressure of grand canonical ensemble is implemented and $\Pi(N)$ is the probability distribution function, which was obtained from previous step.

The critical properties are estimated in order from a least square fit of the law of rectilinear diameter (Van Poolen *et al*. 1997). First, the critical temperature is estimated from the following expression,

$$\rho^l - \rho^v = C_1\left(1-\frac{T}{T_c}\right)^{\beta_c} + C_2\left(1-\frac{T}{T_c}\right)^{\beta_c+\Delta} \tag{5}$$

where $\rho^l$ and $\rho^v$ are the liquid and vapor densities, respectively, and $C_1$ and $C_2$ are fitting parameters. The critical exponent $\beta_c$ is taken as 0.325 and $\Delta = 0.51$. The critical density is then determined from the least square fit to the following expression.

$$\frac{\rho^l + \rho^v}{2} = \rho_c + C_3(T - T_c) \tag{6}$$

where $C_3$ is constant. Finally, critical pressure is estimated using the least square fit to the Clausius-Clayperon expression,

$$\ln P = A + B/T \tag{7}$$

where $A$ and $B$ are constants.

The surface tension is estimated by calculating interfacial free energy, of which the bridge function is expressed as follows,

$$2\beta F_L = \ln\left(\frac{\Pi^V_{Max}\Pi^L_{Max}}{\left(\Pi^I_{Min}\right)^2}\right) \tag{8}$$

where $F_L$ is the interfacial free energy and the subscript $L$ stands for the finite system size (box length $L$), $\Pi^V_{Max}$ and $\Pi^L_{Max}$ are the maximum probabilities in the vapor and liquid regions, respectively, and $\Pi^I_{Min}$ represents the minimum probability in the interface region. Once $F_L$ is obtained, by using Binder's equation (Binder, 1982), the surface tension is determined by the follow equation,

$$\beta\gamma_L = \frac{\beta F_L}{2L^2} = C_1\frac{\ln L}{L^2} + C_2\frac{1}{L^2} + \beta\gamma \tag{9}$$

where $\gamma_L$ is the surface tension of the box length $L$, $\gamma$ is the surface tension in the infinite limit as $L\to\infty$. The number 2 appears due to presence of two surfaces in the simulation, and $C_1$ and $C_2$ are constants. (See Singh *et al*., 2007 for detailed procedure).

**Simulation Details**

The varying parameters are *S* and temperature with a *D* fixed as unity. The range of *S* varies from around 6 to 10, which includes the regime of Lennard-Jones (LJ) potential (at $S \approx 6$). Note that temperature depends on the value of *S*. Our results include the parameters of metallic components, which were previously done by same authors (Singh *et al*., 2006). The maximum numbers of particles vary from 350 to 550. Size effect of the number of particle is minimal in the estimated values in this work. MC trial moves are assigned to be 30 % particle displacement, 35 % particle insertion, and 35 % particle deletion. Typically, the statistical error is found to be less than 1%.

**RESULTS AND DISCUSSIONS**

We first look at coexistence behavior of Morse fluids. Figure 2 shows the phase diagram of Morse fluids of reduced temperature versus reduced density with varying *S*.

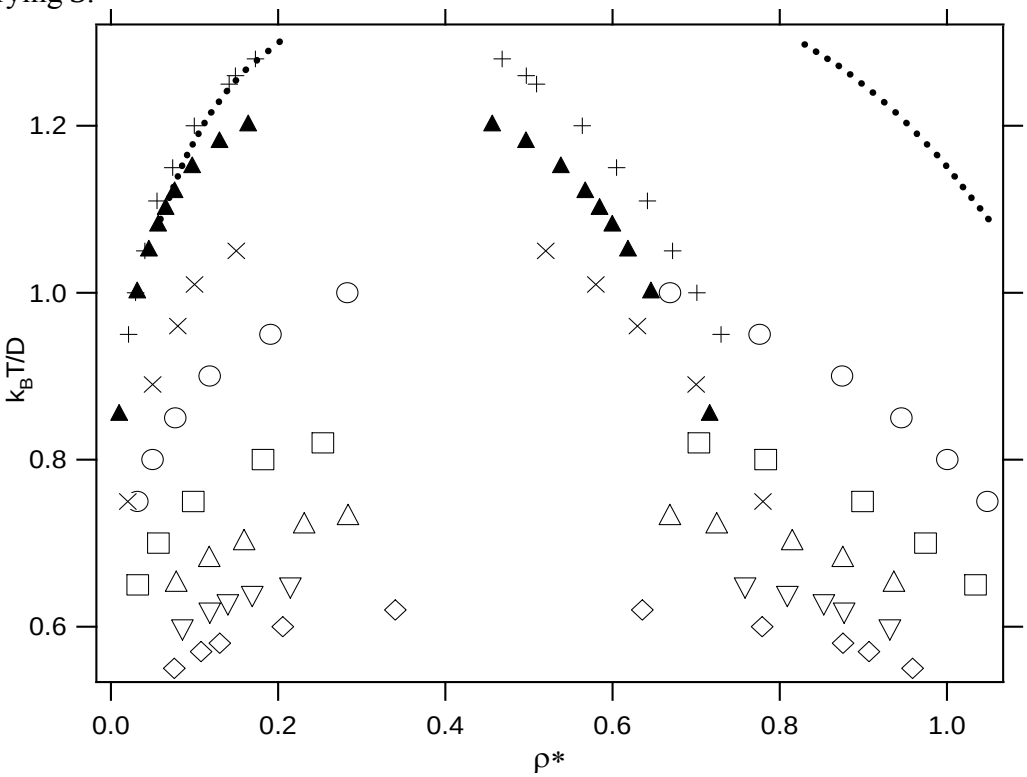


Figure 2. Plot of reduced temperature vs. density. $\rho^*$ is $\rho r_0^3$. Open circle is for *S*=6, open square is for *S*=7, open triangle is for *S*=8, open inverse triangle is for *S*=9, and open diamond is for *S*=10. The dotted line is for *S*=4.87(Singh *et al*., 2006). Filled triangle is for square-well fluids with λ=1.5(Singh *et al*. 2003), the + symbol is for LJ fluids(Potoff and Panagiotopoulos, 2000), and the × symbol is for Buckingham exponential-6 fluids(Errington and Panagiotopoulos, 1998).

DOI: 10.2202/1934-2659.1097 

Note that the dotted line is added to show the phase curve for the metal component, Au (S≈4.87). We also show typical coexistence data of square-well (SW), LJ, Buckingham exponential-6 potentials for comparison. Left region of the plot represents the gas phase and the right region represents the liquid phase. As the parameter *S* increases, the region of phase coexistence decreases as well as the critical temperature. The cause of this behavior can be sought from observing interaction forces between molecules. Once *S* increases, the interactions of molecules become short ranged (narrower potential well; steeper interaction force) so that many particles beyond certain range of interaction distance do not participate. This leads to lower in free energy difference between two phases, consequently results in the decrease of the critical temperature. Similar behavior is being observed for the variable SW systems (Singh *et al*., 2003; Kiselev *et al*., 2006). Figure 3 shows the corresponding state plot of fig. 2.

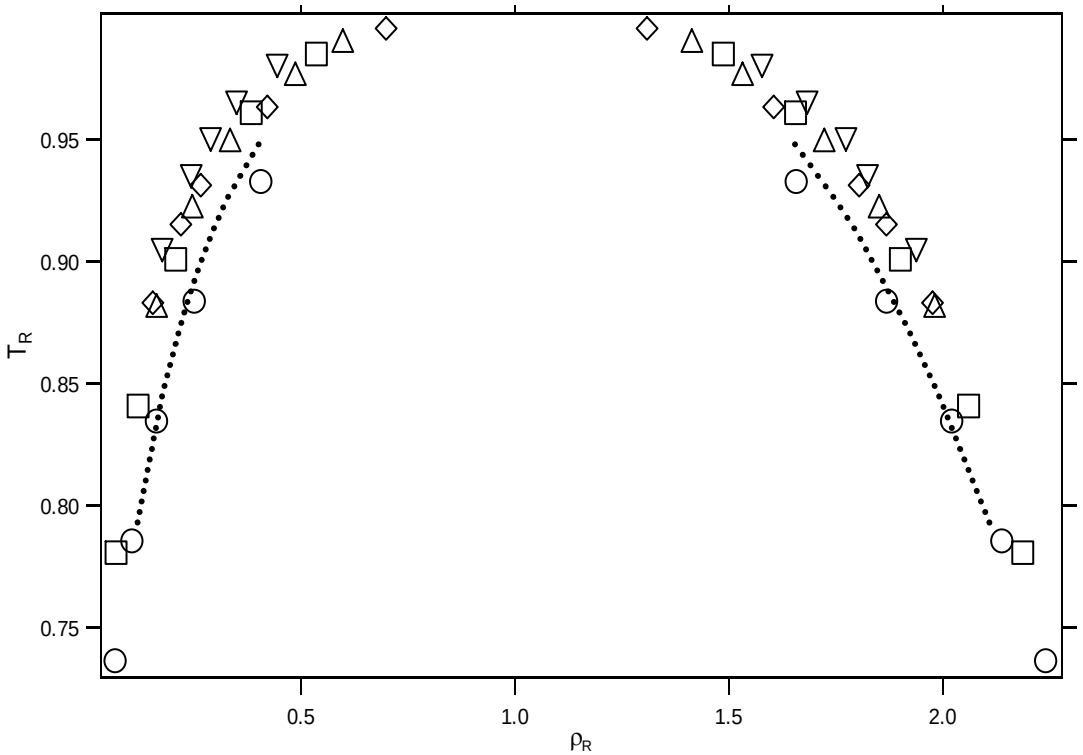


Figure 3. Plot of reduce temperature vs. reduced density, where $T_R = T^*/T_c^*$ and $\rho_R = \rho^*/\rho_c^*$. Open circle is for *S*=6, open square is for *S*=7, open triangle is for *S*=8, open inverse triangle is for *S*=9, and open diamond is for *S*=10. The dotted line is for *S*=4.87(Singh *et al*., 2006).

We observe that all systems under consideration fall into within certain range yet with scattered behavior. We speculate that one of these reasons could be from effects of nonlinear behavior of critical densities. Figure 4 shows the reduced saturation pressure (in logarithmic scale) as a function of inverse temperature. The values of saturation pressure were obtained from the application of Eq.(4). Linear feature of pressure with respect to inverse temperature was observed as shown in Clausius-Clayperon expression of Eq.(7). As *S* increases, saturation temperatures are shifted into lower regime. The linear relation allows predicting the critical pressures if the critical temperatures are known (the calculations are shown later in this work). Alternatively, we estimate the critical temperatures by using Eq.(5) to show the behavior of critical temperature as a function of the parameter *S* shown in fig. 5. We found that there exists a *linear relation* of the critical temperature with respect to the parameter *S* in Morse fluids.

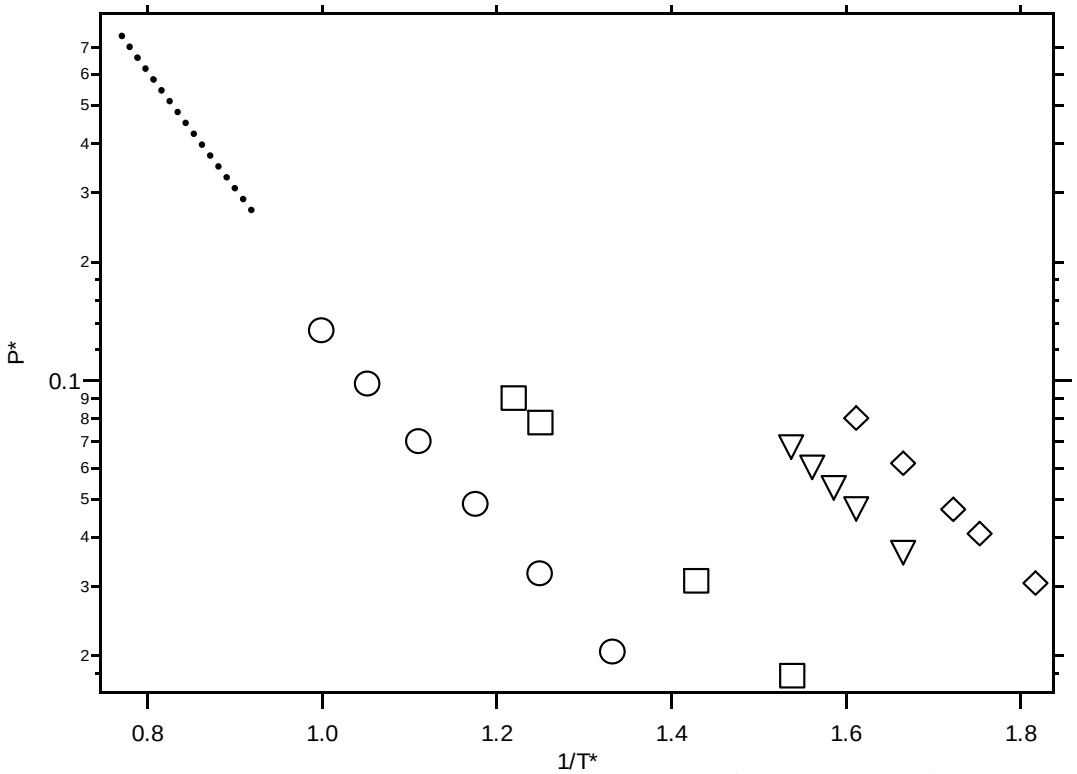


Figure 4. Plot of reduced pressure vs. inverse temperature. $P^*$ is $P\rho^3/D$ and $T^*$ is $k_BT/D$. Open circle is for $S$=6, open square is for $S$=7, open inverse triangle is for $S$=9, and open diamond is for $S$=10. The dotted line is for $S$=4.87(Singh *et al*., 2006).

DOI: 10.2202/1934-2659.1097 

Figure 5 represents our argument. It is found that the linear relation is as follows,

$$1/T_c \approx 1.2\ln(S) - 1.15 \qquad (10)$$

There are two important applications of Eq.(10). One is that if $S$ is given, the critical temperature can be directly estimated. The other provides us the direct limitation of $S$ as $T_c \to \infty$. From Eq.(10), the value of $S$ can be obtained as around 2.6. At this value and lower, phase separation should be under speculation since the attractive interaction become very much long-ranged and repulsive force becomes very weak among molecules; the physical system may depict a conglomerated fluid phase. Therefore, no matter what Morse systems are under consideration, the systems with $S$ below 2.6 can not be considered for phase equilibria determination. On the other hand, the high limit of $S$ is found to be around 50 (work not shown), which approach to limit of short range interaction ($\lambda$=1.1) of SW fluids. In this range, the critical temperature becomes too low and existence of vapor-liquid system is questionable. The opposite behaviors are observed in terms of interaction forces, compared to lower $S$ region.

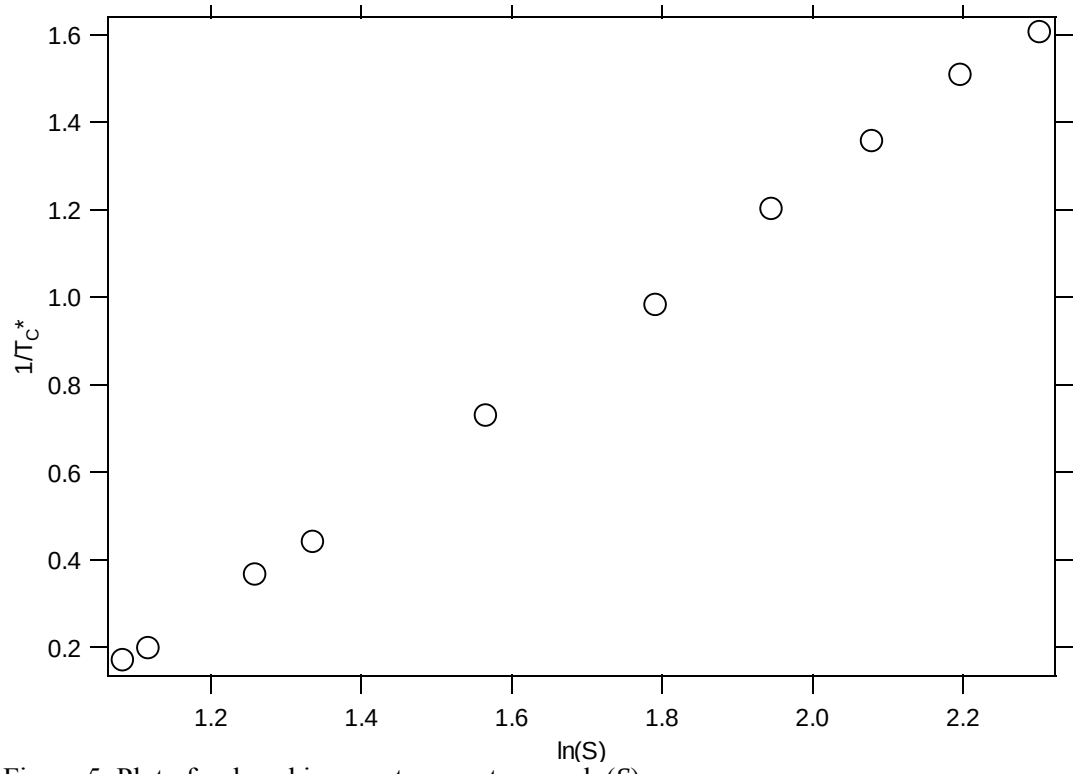


Figure 5. Plot of reduced inverse temperature vs. ln($S$).

With variation of *S*, we did not observe any linear relations with respect to critical pressure and density. The reduced critical properties of the systems of interest are shown in Table 1. As *S* increases, the critical temperature and pressure (with deviation) decrease. However, the critical density does not show any distinct behavior. To predict the critical pressure, we use the data of the saturation pressures (See fig.4) to determine constants of A and B in Eq.(7) and apply the critical temperature estimated from Eq.(5). The critical density was estimated by using Eq.(6).

Surface tension calculations are also performed for the systems of interest. Figure 6 shows the results. We obtain the values by using Eqs. (8) and (9) with finite size scaling method. As temperature increases, the surface tension decreases. We found that surface tension becomes higher with low *S* at a constant temperature. By the same token, the interaction forces between molecules at low *S* become long ranged and those lead to increase in the interfacial free energy.

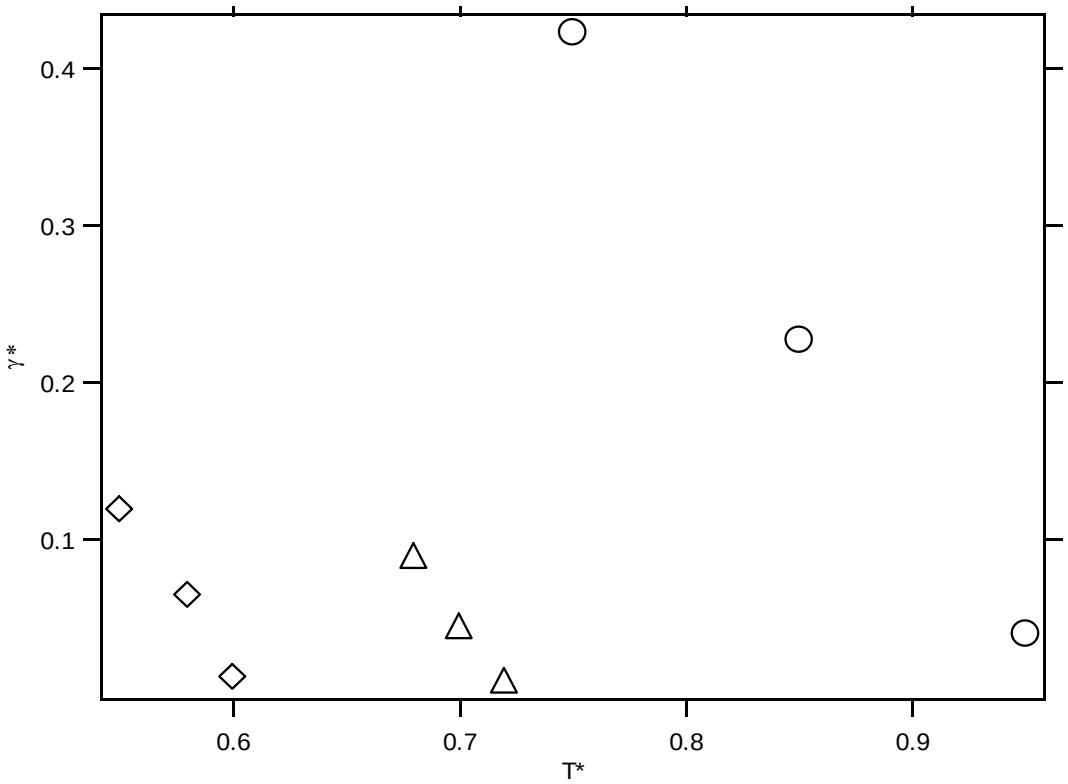


Figure 6. Plot of reduced surface tension vs. temperature, where $\gamma^*$ is $\gamma\varepsilon\sigma^2/D$ and $T^*$ is $k_BT/D$. Open circle is for *S*=6, open triangle is for *S*=8, and open diamond is for *S*=10.

DOI: 10.2202/1934-2659.1097 

## CONCLUSIONS

In this study, we investigated the behavior of Morse fluids in terms of VLE including critical properties. The GC-TMMC with the histogram reweighting method was implemented with other supplementary algorithms such as rectilinear diameter fitting approach and finite scaling method. In Morse formalism, typical variable parameters are $\alpha$ with equilibrium distance $r_0$. Mapping of $\alpha r_0$, which is denoted as parameter $S$, is of great help to reduce the wide range of phase behaviors into small domain, further, to help to find *a linear relation* of the inverse critical temperature with respect to ln($S$). We quantify the relation with lower and upper limits of $S$ of Morse PEF systems, which are found to be around 2.6 and 50, respectively. The range of value $S$ studied in this work is between 6 (which exhibit similar behavior of LJ PEF) and 10.

It is found that as the parameter $S$ increases, the phase coexistence region decreases to lower temperature region. Consequently, critical temperature decreases with $S$. Critical pressure is also noticed to decrease with the increase in $S$. However, such relation was not observed distinctively for critical density. Surface tensions for three sets of $S$ are reported, and those are observed to be increase with the decrease of $S$.

Behaviors of bulk phases and associated critical properties with respect to $S$ are explained in terms of varied potential well of Morse PEF with interaction forces. Small changes of the shape of well may result in big changes in thermodynamic properties and these behaviors were mapped with the parameter $S$.

Complementary work can be undertaken to figure out the clear upper limit of the parameter $S$. Our preliminary investigation shows that the value $S$ is around 50. It indicates typical limit of well-length of SW fluids, for which two phase systems exist(Kiselev *et al*., 2006). Detailed comparison of Morse and SW PEF's might explicitly reveal the upper limit with a varied value of $S$.

## REFERENCES

Binder, K., *Monte Carlo calculation of the surface tension for two- and three-dimensional lattice-gas models*, Phys. Rev. A, 1982, 25, 1699.

Errington, J.R., *Evaluating Surface Tension using grand-canonical transition-matrix Monte Carlo simulation and finite-size scaling*, Phys. Rev. E, 2003, 67, 012102.

Errington, J.R. and Panagiotopoulos, A.Z., *Phase equilibria of the modified Buckingham exponential-6 potential from Hamiltonian scaling grand canonical Monte Carlo*, J. Chem. Phys., 1998, 109, 1093.

Girifalco , L.A. and Weizer, V.G., *Application of the Morse Potential Function to Cubic Metals*, Phys. Rev., 1959, 114, 687.

Ferrenberg, A.M. and Swendsen, R.H., *New Monte Carlo technique for studying phase transitions*, Phys. Rev. Lett., 1988, 61(23), 2635.

Keyes, R.W., *Morse Potentials for Excited States of Diatomic Molecules*, J. Chem. Phys., 1958, 29, 523.

Kiselev, S.B., Ely, J.F. and Elliott JR, J.R., *Molecular dynamic simulations and global equation of state of square-well fluids with the well-widths from lambda=1.1 to 2.1*, Mol. Phys., 2006, 104, 2545.

Lincoln, R.C., Koliwad, K.M., and Ghate, P.B., *Morse-Potential Evaluation of Second- and Third-Order Elastic Constants of Some Cubic Metals*, Phys. Rev., 1967, 157(3), 463.

Morse, P.M., *Diatomic Molecules According to the Wave Mechanics. II. Vibrational Levels*, Phys. Rev., 1929, 34, 57.

Van Poolen, L.J., Holcomb, C.D., and Niesen, V.G., *Critical temperature and density from liquid-vapor coexistence data: application to refrigerants R32, R124, and R152a*, Fluid Phase Equil., 1997, 129(1-2), 105.

Potoff, J.J., and Panagiotopoulos, A.Z., *Surface tension of three-dimension Lennard-Jones fluid from histogram-reweighting Monte Carlo simulations*, J. Chem. Phys., 2000, 112, 6411.

Ruffa, A.R., *Thermal expansion and melting in cubic crystals*, Phys. Rev. B, 1981, 24(12), 6915.

Singh, J.K., Adhikari, J., and Kwak, S.K., *Vapor-liquid phase coexistence curves for Morse fluids*, Fluid. Phase Equil., 2006, 248, 1-6; *Interfacial Properties of Morse Fluids*, Mol. Phys., 2007, 105, 981.

Singh, J.K., Errington, J.R., and Kofke, D.K., *Surface tension and vapor-liquid phase coexistence of the square-well fluid*, J. Chem. Phys., 2003, 119, 3405.

DOI: 10.2202/1934-2659.1097 